ARMY RESEARCH LABORATORY

Modeling of a Fluid Breakup Through Nonlinear Fluid Flow: Description of Methodology

by Josip Z. Šoln

ARL-TR-2543

June 2001

Army Research Laboratory
Aberdeen Proving Ground, MD 21005-5423

ARL-TR-2543 **June 2001**

Modeling of a Fluid Breakup Through Nonlinear Fluid Flow: Description of Methodology

Josip Z. Šoln
Survivability/Lethality Analysis Directorate, ARL

Abstract

Employing the Galerkin method, we find altogether four solutions for the Navier-Stokes equation describing the airflow around a fluid sphere. Two solutions are real, and two are complex. Of the two real solutions, one is a standard solution described by Kawaguti some time ago. A new real solution is distinctly different from the standard one and, as such, gives a qualitatively different description of the flow around a sphere. For large Reynolds numbers, this new solution should be appropriate for deducing the critical forces on the fluid sphere responsible for its breakup.

Table of Contents

INTENTIONALLY LEFT BLANK.

List of Figures

INTENTIONALLY LEFT BLANK.

List of Tables

INTENTIONALLY LEFT BLANK.

Executive Summary

In support of the Air Defense Intercept effort, the author proposes to model the fluid breakup through the Navier-Stokes equation by studying the flow instability around the spherical fluid at very high air velocities. Essentially, the air treated here as a fluid exhibits highly nonlinear behavior. The breakup of the spherical fluid is to be connected to secondary flow and flow instability of the air around the spherical fluid. In addition to the standard real Galerkin method solution of the Navier-Stokes equation, valid mostly for small Reynolds numbers, a new real Galerkin method solution has also been found. It is distinctly different from the standard one and, therefore, should be capable of describing the flow at large Reynolds numbers. As such, it is appropriate for deducing the breakup of the ejected fluid.

INTENTIONALLY LEFT BLANK.

1. Introduction

1.1 Purpose. The purpose of this report is to describe and illustrate the numerical Galerkin method solution of the Navier-Stokes equation as applied to the breakup of an agent released from a missile.

1.2 Background. After a dense fluid is ejected by the impact from the intercept, it travels at very high (most often, sonic) speeds through the air. In what follows, the author assumes, to a good approximation, that the ejected fluid is of a spherical shape. However, the secondary flow and flow instability of the air (treated here as a fluid) around the spherical fluid believed to be responsible for the fluid breakup represents a highly nonlinear problem when being tackled by the Navier-Stokes equation. The flow (velocity) field can be computed in one of the two ways: by numerical methods seeking a solution for velocities only at a set of selected grid points in the flow region, or by the Galerkin method, in which the solution of the flow field is approximated by a continuous function expanded in terms of polynomials with arbitrary coefficients. Regardless of whether the numerical or the Galerkin method is used, the fact that the dense fluid is assumed to be of spherical shape should be helpful when formulating the problem through the Navier-Stokes equation for the motion of air as a fluid around it.

1.2.1 General. For the description of the air streaming around the spherically shaped high-density fluid (Figure 1), the form of the Navier-Stokes equation as originally given by Hughes and Gaylord [1] is particularly useful Then, choosing the origin of the spherical coordinates at the center of the sphere, an assumption can be made that far away from the sphere the flow is of a constant speed U along the z-axis. It is easily seen that the z-axis represents axis of axial symmetry; the flow (velocity) field is independent of the azimuthal angle (coordinate) ϕ. In essence, there are only two independent velocity components—u_r, the radial component and u_θ, the angular component. For such an axisymmetric configuration for which the velocity flow field is independent of ϕ, a Stoke's scalar stream function ψ can be introduced, which, in turn, determines u_r and u_θ.

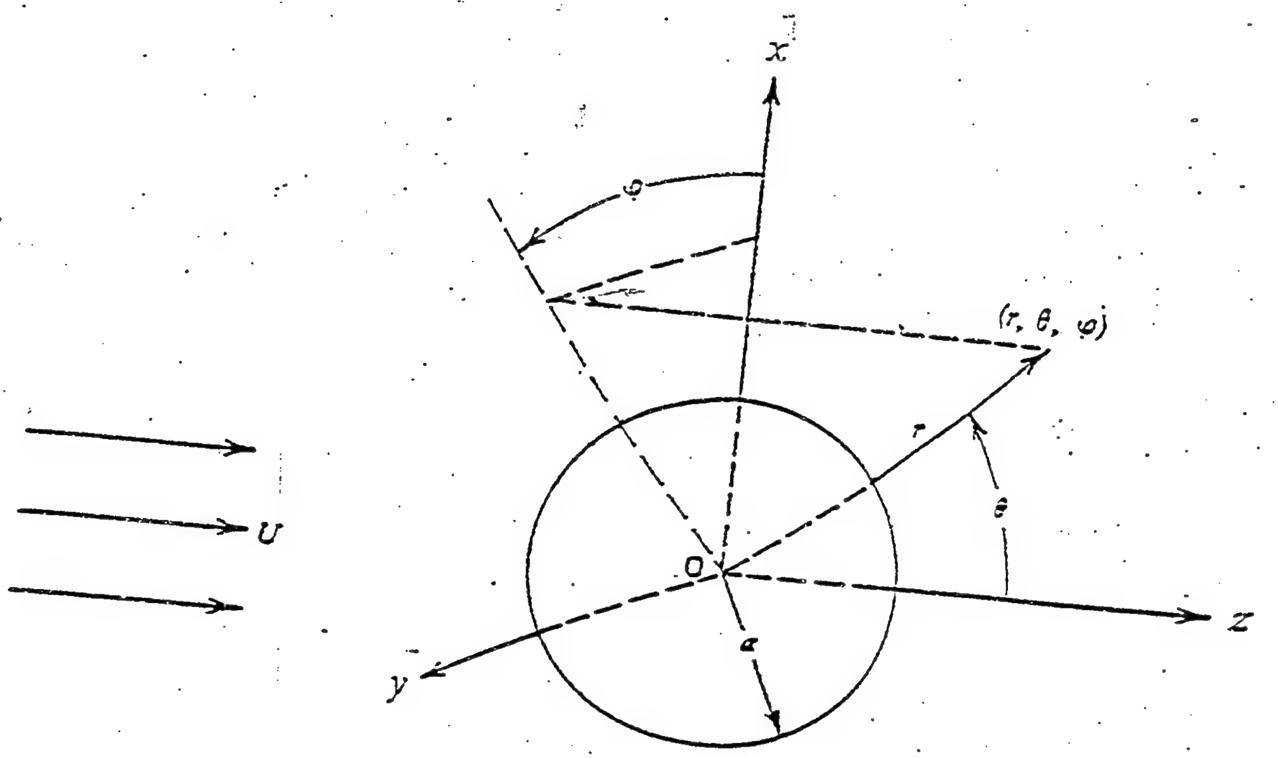

Figure 1. Representation of the Coordinate System With the Origin in the Center of a Fluid Sphere Traveling With Very High (Sonic) Speeds Through the Air.

The boundary conditions must be taken into account properly and are actually quite simple. The velocity components u_r and u_ϕ must be both zero on the sphere, and the flow far away from the sphere must be uniform. These boundary conditions are now easily translated to the Stokes scalar stream function ψ.

The Navier-Stokes equation in the form of Hughes and Gaylord [1] is now rewritten for the Stokes scalar stream function ψ. Although, instead of two vector field components, u_r and u_θ, there is now a differential equation for just one scalar function ψ. Even so, this is still a very complicated differential equation, quadratic both in differential operators and the function ψ.

Specializing now to the Galerkin method, ψ must be expanded in terms of a complete set of basic functions $F_i(r,\xi)$, where r is the radial distance and $\xi = \cos\theta$. In order to satisfy the boundary conditions, the simplest approach is to make $F_i(r,\xi)$ a linear combination of the Legendre polynomials, $P_l(\xi)$, where the coefficients in the expansion a_i (r) are still functions of the radial distance r.

Determining the coefficients $a_i(r)$ is actually a very difficult task, except in simplified special situations. When determining these coefficients on the sphere, the Navier-Stokes equation must be satisfied exactly for approximated ψ; away from the sphere, there is generally an error. The demand that the distribution of this error throughout the flow field vanish, at least in principle, supplies a set of algebraic equations. Finding the solution of these equations is a major task and it can be done; the solutions, once found, determine the expansion coefficients. This, in turn, gives the approximated ψ, which then becomes a known function of r and θ.

Having obtained the stream function ψ, many properties of the flow around the sphere can be deduced (i.e., the flow pattern since it is now easy to obtain the velocity components u_r and u_θ, as well as their derivatives). However, to find out under which conditions (e.g., at which air speeds) the sphere starts to break up, the drag of the sphere must be computed. This can be done with the help of the normal and shear stresses which are given in terms of the derivatives of air velocity components at the surface of the sphere. In any case, the drag of the sphere consists of two parts: D_p, the pressure drag (also known as the form drag) caused by the normal stresses and D_s, the skin friction caused by shear stress on the surface of the sphere. To evaluate D_p, the pressure which can be obtained in principle from the Navier-Stokes equation in the Hughes and Gaylord form [1] must be known.

1.2.2 Threat. The methodology presented in this report addresses the effects of agent-fluid break-up threats on soldiers and a military weapon system from both ballistic and cruise missiles.

1.3 Scope. The scope of this report is to utilize a physics approach to solving and understanding problems of fluid breakup associated with ballistic and cruise missiles.

2. Theoretical Formulation of the Method

It can be assumed that for a hurling airborne spherical fluid, the air itself, as long as there are no additional forces acting on the system, to a good approximation, is incompressible; that is, its density is practically constant in time, which means:

$$\frac{D\rho}{Dt} = 0, \frac{D}{Dt} = \frac{\partial}{\partial t} + \vec{u} \cdot \nabla .$$

Owing to the continuity equation,

$$\frac{1}{\rho}\frac{D\rho}{Dt} + \nabla \cdot \vec{u} = 0. \tag{1}$$

This means that the velocity of the air-fluid element is divergenceless:

$$\nabla \cdot \vec{u} = 0 . \tag{2}$$

The origin of the spherical coordinate system (r, θ, ϕ) is situated at the center of the fluid sphere, whose radius is a (Figure 1). Far away, the flow of the air is of constant speed and, by definition, in the z-direction, $\vec{u} = \hat{z}U$. Furthermore, the axisymmetric configuration (the velocity flow field of the air around the fluid sphere is independent of ϕ) is exploited. For such a flow, a Stokes stream scalar function ψ is introduced, which, in turn, defines the r and θ components of the velocity as

$$u_r = \frac{1}{r^2 \sin\theta}\frac{\partial\psi}{\partial\theta} = -\frac{1}{r^2}\frac{\partial\psi}{\cos\theta} \tag{3}$$

and

$$u_\theta = -\frac{1}{r\ \sin\theta}\frac{\partial\psi}{\partial r}. \tag{4}$$

In what follows, the form of the incompressible Navier-Stokes equation as given by Hughes and Gaylord [1] is utilized as follows:

$$\rho\left[\frac{\partial\vec{u}}{\partial t} - \vec{u}\times(\nabla\times\vec{u})\right] = -\nabla\left(p + \frac{1}{2}\rho\ \vec{u}^{\,2}\right) - \mu\nabla\times(\nabla\times\vec{u}), \tag{5}$$

where μ is the kinematic viscosity of the air.

As mentioned in section 2, a very important and rather helpful quantity when trying to solve equation (5) is the dimensionless Reynolds number R_e, defined generally as

$$R_e = \frac{UL}{\nu},\ \mu = \nu\rho\,, \tag{6}$$

where U and L denote a typical flow speed and a characteristic length scale, respectively [2]. For example, for air flowing around the dense fluid sphere, L = 2a, where a is the radius of the sphere. U, of course, is simply the magnitude of the incoming velocity of the air toward the sphere. Equation (6) shows the connection between the ordinary (μ) and the kinematic (ν) viscosity, where ρ is the density of the fluid, the air in our case.

Already from equation (5), the usefulness of the Reynolds number can be seen by estimating the orders of magnitudes for inertia and viscous terms. Namely, from

$-\rho\bar{u}\times(\nabla\times\bar{u}) = -(\rho/2)\nabla\bar{u}^2 + \rho(\bar{u}\cdot\nabla)\bar{u}$, the inertia term is identified with $\rho(\bar{u}\cdot\nabla)\bar{u}$ while, on the other hand, from $-\mu\nabla\times(\nabla\times\bar{u}) = -\mu\nabla(\nabla\cdot\bar{u}) + \mu\nabla^2\bar{u} = \mu\nabla^2 u$, the viscous term is identified with $\mu\nabla^2\bar{u}$. Assuming now that the derivatives of the velocity components typically change by amounts of order U/L over distances of order L, the following order of magnitude estimates for the inertia and viscous terms in equation (5) are obtained:

$$\text{inertia term: } \rho\left|(\bar{u}\cdot\nabla)\bar{u}\right| = \rho O(U^2/L), \tag{7}$$

and

$$\text{viscous term: } \left|\mu\nabla^2\bar{u}\right| = \mu O(U/L^2). \tag{8}$$

Hence, it can be deduced that

$$\frac{|\text{inertia term}|}{|\text{viscous term}|} = O\left(\frac{U^2/L}{\nu U/L^2}\right) = O(R_e). \tag{9}$$

So, it can be seen immediately that $R_e >> 1$ corresponds to the motion of fluid of small viscosity and/or large L. However, $R << 1$ does not always mean the motion of fluid of large viscosity; $R << 1$ can also be achieved with small L.

With the assumption of steady flow ($\partial\bar{u}/\partial t = 0$), after taking the curl of both sides of the equation (variations of p and ρ with respect to space and time are assumed to be negligible), and taking into account equations (3) and (4), one obtains the following equation for ψ:

$$\frac{1}{r^2\sin\theta}\left(\frac{\partial\psi}{\partial\theta}\frac{\partial}{\partial r} - \frac{\partial\psi}{\partial r}\frac{\partial}{\partial\theta} + 2\cot\theta\frac{\partial\psi}{\partial r} - \frac{2}{r}\frac{\partial\psi}{\partial\theta}\right)D^2\psi = \frac{2}{R_e}D^4\psi, \tag{10}$$

where the operator D^2 is defined as

$$D^2 = \frac{\partial^2}{\partial r^2} + \frac{\sin\theta}{r^2}\frac{\partial}{\partial\theta}\left(\frac{1}{\sin\theta}\frac{\partial}{\partial\theta}\right). \tag{11}$$

As usual, the Reynolds number based on the diameter of the sphere is

$$R_e = \frac{2\rho Ua}{\mu}. \tag{12}$$

Now, it is clear that the velocity of the air-fluid element depends on r and θ; as such, it should vanish at the surface of the sphere. Therefore,

$$\psi(a,\theta) = 0, \tag{13}$$

and

$$\frac{\partial\psi}{\partial r}(a,\theta) = 0. \tag{14}$$

Furthermore, away from the sphere $r \to \infty$, it is obtained from equation (10) that

$$D^2\psi(r,\theta) = 0 \text{ as } r \to \infty, \tag{15}$$

implying that

$$\psi(r,\theta) = \frac{U}{2} r^2 \sin^2\theta \text{ as } r \to \infty, \tag{16}$$

which is the statement that the flow far away from the body is uniform; U is the initial velocity of the air in the z-direction.

Equations (13), (14), and (16) have to be satisfied throughout the calculations; in fact, these equations practically require the use of Legendre polynomials when expanding ψ in terms of a complete set of basic functions.

Without actually solving the problem numerically and/or analytically, the behavior of the fluid sphere in the air at very high velocities can be addressed. Namely, at small Reynolds numbers, R_e, the drag of the sphere is dominated by the skin friction; while for $R_e > 90$, the pressure drag becomes more important. Since R_e increases as the velocity around the sphere increases, this means that the pressure is rather important in the breakup of the fluid at higher air velocities. Now one can proceed phenomenologically to determine how the breakup of the fluid sphere is related to drag, pressure stress, shear stress, or the pressure itself; however, this may take some time to figure out.

3. Implementation of the Galerkin Method to Solve the Navier-Stokes Equation for Finite Reynolds Numbers

As mentioned earlier, the calculations are easier to track if we use the new variable

$$\xi = \cos\theta. \tag{17}$$

With this variable, the nonlinear differential equation from (10) now becomes

$$\frac{2}{R_e} D^4\psi + \frac{1}{r^2}\left(\frac{\partial\psi}{\partial\xi}\frac{\partial}{\partial r} - \frac{\partial\psi}{\partial r}\frac{\partial}{\partial\xi} - \frac{2\xi}{1-\xi^2}\frac{\partial\psi}{\partial r} - \frac{2}{r}\frac{\partial\psi}{\partial\xi}\right)D^2\psi = 0, \tag{18}$$

where now

$$\psi = \psi(r,\xi) \tag{19}$$

and

$$D^2 \equiv \frac{\partial^2}{\partial r^2} + \frac{1-\xi^2}{r^2}\frac{\partial^2}{\partial \xi^2}. \tag{20}$$

Furthermore,

$$D^2\psi = 0 \text{ as } r \to \infty \tag{21}$$

yields

$$\psi(r,\xi) = \frac{U}{2} r^2 (1-\xi^2) \text{ as } r \to \infty. \tag{22}$$

Now, the Galerkin method demands that the solution to equation (18) or equivalently to equation (10) be approximated by a polynomial formed from a set of some basic functions. Taking into account equations (13–16) and (22), it is not difficult to see that these basic functions should involve the Legendre polynomials, defined here by Rodrigues' formula [3]:

$$P_m(\xi) = \frac{1}{2^m m!}\frac{d^m}{d\xi^m}(\xi^2 - 1)^m. \tag{23}$$

A few quotes follow:

- $P_0(\xi) = 1$.
- $P_1(\xi) = \xi$.
- $P_2(\xi) = \frac{1}{2}\left(3\xi^2 - 1\right)$.

- $P_3(\xi) = \frac{1}{2}\left(5\xi^3 - 3\xi\right)$.
- $P_4(\xi) = \frac{1}{8}\left(35\xi^4 - 30\xi^2 + 3\right)$.

The basic functions $F_i(r,\xi)$ are chosen in the following form [1, 4]:

$$F_i(r,\xi) = f_i(r)\left[P_{i-1}(\xi) - P_{i+1}(\xi)\right], \tag{24}$$

where, due to orthogonality of the Legendre polynomials, the orthogonality of $F_i(r,\xi)$ is

$$\int_{-1}^{1} F_i(r,\xi)F_j(r,\xi)d\xi \approx \delta_{ij}. \tag{25}$$

The solution is simply approximated by the following linear combination:

$$\frac{\psi(r,\xi)}{U} = \sum_{i=1}^{n} F_i(r,\xi). \tag{26}$$

As already argued by Kawaguti [4], it should be possible now to choose the coefficients $f_i(r)$ in such a way that while the solution in equation (26) is only approximate, all the boundary conditions are satisfied exactly.

For example, $f_1(r) = r^2/3$ reproduces ψ in form (equation [22]); however, other terms are clearly needed, as otherwise conditions in equations (13) and (14) cannot be satisfied [4]. The simplest condition to satisfy equation (13) is to change $f_1(r) = r^2/3$ into $\left(r^2/3\right)\left(1 - a/r\right)$, which also satisfies conditions in equations (13) and (22). Unfortunately, even for $n = 2$, the condition in equation (14) is not satisified; more terms as a power series in r^{-1} are needed [4].

With Kawaguti [4], $n = 2$ is chosen because

$$P_0(\xi) - P_2(\xi) = \frac{3}{2}\left(1-\xi^2\right) \tag{27}$$

and

$$P_1(\xi) - P_3(\xi) = \frac{5\xi}{2}\left(1-\xi^2\right). \tag{28}$$

We write for ψ

$$\psi = Ua^2\left\{\begin{array}{l}\left[\dfrac{1}{2}\rho^2 + \left(\dfrac{A_1}{\rho}+\dfrac{A_2}{\rho^2}+\dfrac{A_3}{\rho^3}+\dfrac{A_4}{\rho^4}\right)\right]\left(1-\xi^2\right) \\ +\left(\dfrac{B_1}{\rho}+\dfrac{B_2}{\rho^2}+\dfrac{B_3}{\rho^3}+\dfrac{B_4}{\rho^4}\right)\xi\left(1-\xi^2\right)\end{array}\right\} \tag{29}$$

and

$$\rho \equiv \frac{r}{a}. \tag{30}$$

Equation (29) automatically satisfies the boundary condition in equation (22) of uniform flow at infinity. The two conditions in equations (13) and (14) at the surface require

$$\sum_{i=1}^{4} A_i = -\frac{1}{2}, \tag{31}$$

$$\sum_{i=1}^{4} B_i = 0, \tag{32}$$

$$\sum_{i=1}^{4} i\,A_i = 1, \tag{33}$$

and

$$\sum_{i=1}^{4} iB_i = 0 . \tag{34}$$

For later use, the following identities are from equations (32–35):

$$\sum_{i=1}^{4} (2+i)A_i = 0, \tag{35}$$

and

$$\sum_{i=1}^{4} (3+i)B_i = 0. \tag{36}$$

The next step is to substitute equations (29) and (30) into equation (18), starting with just A_1, A_2, B_1, and B_2 while assuming, at least temporarily, that the rest of coefficients are zero. It is easily seen that this is not sufficient. Equations (31–36) are solved exactly to yield $A_1 = -2$, $A_2 = 3/2$, and $B_1 = B_2 = 0$ and, as such, give a solution for ψ. However, when this is substituted into equation (18), the error is just too big and impossible to eliminate since the coefficients have already been determined. Thus, it is best to assume that all A's and B's from equations (29) and (30) are different from zero. The author may, however, later try to see what happens if some of them (e.g., A_4 and B_4) are put to zero. Substituting with these coefficients for ψ into equation (18), an error denoted [1, 2, 4] as [NS] is obtained on the left-hand side of the Navier-Stokes equation:

$$[NS] = (1-\xi^2)[G_0(\rho) + \xi G_1(\rho) + \xi^2 G_2(\rho) + \xi^3 G_3(\rho) + (1-3\xi^2)(E_0(\rho) + \xi E_1(\rho))], \tag{37}$$

denoting

$$a_n = \frac{A_n}{\rho^n} \quad \text{and} \quad b_n = \frac{B_n}{\rho^n}. \tag{38}$$

Functions in equation (37) are expressed as follows:

$$G_0(\rho) = \frac{4}{\rho^5}\left[\frac{2}{R_e}\rho\left(9a_2 + 35a_3 + 90a_4\right) - \left(2a_2 + 5a_3 + 9a_4\right)\left(\sum_{i=1}^{4} b_i\right)\right], \tag{39}$$

$$G_1(\rho) = \frac{4}{\rho^5}\left[\begin{array}{l} -\dfrac{6}{R_e}\rho\left(b_1 - 6b_3 - 21b_4\right) + \left(\dfrac{\rho^2}{2} + \displaystyle\sum_{i=1}^{4} a_i\right)\left(12a_2 + 35a_3 + 73a_4\right) \\ + \left(\displaystyle\sum_{i=1}^{4} b_i\right)\left(2b_1 - 3b_3 - 7b_4\right) \end{array}\right], \tag{40}$$

$$G_2(\rho) = \frac{4}{\rho^5}\left[\begin{array}{l} \left(\dfrac{\rho^2}{2} + \displaystyle\sum_{i-1}^{4} a_i\right)\left(-6b_1 + 15b_3 + 42b_4\right) + \left(\displaystyle\sum_{i=1}^{4}(2+i)a_i\right)\left(-2b_1 + 3b_3 + 7b_4\right) \\ + 3\left(2a_2 + 5a_3 + 9a_4\right)\left(\displaystyle\sum_{i=1}^{4} b_i\right) \end{array}\right], \tag{41}$$

$$G_3(\rho) = -\frac{4}{\rho^5}\left(\sum_{i=1}^{4}(3+i)b_i\right)\left(2b_1 - 3b_3 - 7b_4\right), \tag{42}$$

$$E_0(\rho) = \frac{2}{\rho^5}\left[\left(\rho^2 - \sum_{i=1}^{4} i\,a_i\right)\left(2b_1 - 3b_3 - 7b_4\right) - \left(8a_2 + 25a_3 + 54a_4\right)\left(\sum_{i=1}^{4} b_i\right)\right], \tag{43}$$

and

$$E_1(\rho) = \frac{2}{\rho^5}\left[\left(\sum_{i=1}^{4} b_i\right)\left(6b_1 - 15b_3 - 42b_4\right) - \left(\sum_{i=1}^{4} i\,b_i\right)\left(2b_1 - 3b_3 - 7b_4\right)\right]. \tag{44}$$

First, the Navier-Stokes equation is satisfied exactly on the sphere by the approximation for ψ, equations (29) and (30). Remember that when $r \to a$, $\rho \to 1$, so that $a_i \to A_i$ and $b_i \to B_i$ which, with the help of equations (31–36), demands:

$$9A_2 + 35A_3 + 90A_4 = 0, \tag{45}$$

and

$$B_1 - 6B_3 - 21B_4 = 0\,. \tag{46}$$

With Kawaguti [4], in order to minimize the error, [NS] is expanded in terms $F_i(\rho,\xi)$ from equation (24) with $f_i(\rho) = \rho^{-i}$, and each term must be zero. This is achieved if each coefficient in the expansion is zero; for $n = 2$, these conditions are obtained:

$$\int_1^\infty d\rho\, \rho^{-1} \int_{-1}^{1} d\xi \left(P_0(\xi) - P_2(\xi)\right)[NS](\rho,\xi) \equiv NS1 = 0\,, \tag{47}$$

and

$$\int_1^\infty d\rho\, \rho^{-2} \int_{-1}^{1} d\xi \left(P_1(\xi) - P_3(\xi)\right)[NS](\rho,\xi) \equiv NS2 = 0\,. \tag{48}$$

The integrals in equations (47) and (48), although tedious, are nevertheless straightforward to carry out. To facilitate this, the following functions are defined:

$$f_i(\xi) = \xi^i\,(1-\xi^2),\ i = 0,1,2,3; \tag{49}$$

and

$$h_i(\xi) = \xi^i(1-\xi^2)(1-3\xi^2),\ i = 0,1. \tag{50}$$

Then from equations (47) and (48), it is easily seen that in variable ξ, the following integrals are needed:

$$If_{i02} = \int_{-1}^{1} d\xi\, f_i(\xi)\left(P_0(\xi) - P_2(\xi)\right), \tag{51}$$

$$If_{i13} = \int_{-1}^{1} d\xi\, f_i(\xi)\left(P_1(\xi) - P_3(\xi)\right), i = 0,1,2,3, \tag{52}$$

$$Ih_{i02} = \int_{-1}^{1} d\xi\, h_i(\xi)\left(P_0(\xi) - P_2(\xi)\right), \tag{53}$$

and

$$Ih_{i13} = \int_{-1}^{1} d\xi\, h_i(\xi)\left(P_1(\xi) - P_3(\xi)\right), i = 0,1. \tag{54}$$

All are zero except for the following:

$$If_{002} = 8/5,\ If_{202} = 8/35, \tag{55}$$

$$If_{113} = 8/21, If_{313} = 8/63; \tag{56}$$

and

$$Ih_{002} = 32/35. \tag{57}$$

Integrals in ρ must be calculated. They are defined as follows:

$$IG_{i1} = \int_1^\infty d\rho \; G_i(\rho)\rho^{-1}, \;\; i = 0,1,2,3, \tag{58}$$

$$IG_{i2} = \int_1^\infty d\rho \; G_i(\rho)\rho^{-2}, \;\; i = 0,1,2,3; \tag{59}$$

$$IE_{i1} = \int_1^\infty d\rho \; E_i(\rho)\rho^{-1}, \;\; i = 0,1, \tag{60}$$

and

$$IE_{i2} = \int_1^\infty d\rho \; E_i(\rho)\rho^{-2}, \;\; i = 0,1. \tag{61}$$

In these notations, equations for NS1 and NS2 (equations [47] and [48], respectively) are now written as follows:

$$NS1 = If_{002}IG_{01} + If_{102}IG_{11} + If_{202}IG_{21} + If_{302}IG_{31} + Ih_{002}IE_{01} + Ih_{102}IE_{11} = 0, \tag{62}$$

and

$$NS2 = If_{013}IG_{02} + If_{113}IG_{12} + If_{213}IG_{22} + If_{313}IG_{32} + Ih_{013}IE_{02} + Ih_{113}IE_{12} = 0. \tag{63}$$

These integrals from equations (52–61) have been evaluated using the third edition of Mathematica [5], yielding finally for NS1 and NS2 the following:

$$
\begin{aligned}
NS1 = &-\frac{8\left[2880A_1+7\left(-45+1035A_2+1960A_3+3204A_4\right)\right]B_1}{11025}-\frac{32A_3B_2}{5}\\
&-\frac{4608A_4B_2}{385}+\frac{8B_3}{35}+\frac{64A_1B_3}{21}-\frac{64A_3B_3}{35}-\frac{232A_4B_3}{35}+\frac{32B_4}{35}+\frac{176A_1B_4}{25}\\
&+\frac{56A_3B_4}{15}-\frac{128A_4B_4}{455}+\frac{64A_3}{R_e}+\frac{144A_4}{R_e}\\
&-\frac{16A_2\left(-1386+176B_2R_e-99B_3R_e-444B_4R_e\right)}{1155R_e}=0;
\end{aligned}
\tag{64}
$$

$$
\begin{aligned}
NS2 = &\frac{64A_2^2}{35}+\frac{40A_3^2}{9}+\frac{146A_4}{21}+\frac{2336A_1A_4}{231}+\frac{1168A_4^2}{147}+\frac{16A_3}{273}\left(65+91A_1+216A_4\right)\\
&+\frac{8A_2}{693}\left(132+176A_1+564A_3+935A_4\right)-\frac{8B_1^2}{63}-\frac{128B_1B_2}{567}-\frac{16B_1B_3}{105}+\frac{64B_2B_3}{231}\\
&+\frac{8B_3^2}{21}-\frac{32B_1B_2}{693}+\frac{16B_2B_4}{27}+\frac{352B_3B_4}{273}+\frac{64B_4^2}{63}-\frac{32B_1}{21R_e}+\frac{48B_3}{R_e}+\frac{64B_4}{3R_e}=0.
\end{aligned}
\tag{65}
$$

Equations (31–34), (45), (46), (64), and (65) are the eight equations necessary to solve for the coefficients $A_1, A_2, A_3, A_4, B_1, B_2, B_3, \text{and } B_4$. Unlike equations (31–36), (45), and (46), which are linear, equations (64) and (65) are quadratic in these coefficients; this fact makes solving these equations simultaneously rather difficult. Nevertheless, equations (31–36), (45), and (46) are solved expressing six of the coefficients first in terms of A_1 and B_1 and then, as an exercise, a different set of six coefficients in terms of A_4 and B_4. The results are as follows:

$$
\begin{aligned}
&A_2 = -\frac{15}{29}(8+5A_1),\ A_3 = \frac{9}{29}(17+7A_1),\ A_4 = -\frac{1}{58}(95+34A_1),\\
&B_2 -\frac{23}{9}B_1,\ B_3 \frac{19}{9}B_1,\ B_4 -\frac{5}{9}B_1;
\end{aligned}
\tag{66}
$$

or

$$
\begin{aligned}
&A_1 = -\frac{1}{34}(95+58A_4),\ A_2 = \frac{15}{34}(7+10A_4),\ A_3 = -\frac{9}{34}(3+14A_4),\\
&B_1 = -\frac{9}{5}B_4,\ B_2 = \frac{23}{5}B_4,\ B_3 = -\frac{19}{5}B_4.
\end{aligned}
\tag{67}
$$

Utilizing equation (66) and substituting it into expressions of $NS1$ and $NS2$, equations (64) and (65), explicit expressions are obtained for them as follows:

$$NS1(A_1, B_1, R_e) = -\frac{4(-401625 + 87302A_1)B_1}{137162025} + \frac{72(9 + 2A_1)}{29R_e}, \tag{68}$$

and

$$NS2(A_1, B_1, R_e) = \frac{1}{64438719345R_e} \left[70916685840B_1 + 3645(6413185 + 756034A_1 + 32880A_1^2)R_e - 24207344B_1^2R_e\right], \tag{69}$$

which, when solved formally, yield

$$NS1 = 0: \; A_1 = \frac{4725(162162 + 85B_1\,Re)}{-170270100 + 87302B_1\,Re}, \tag{70}$$

$$NS2 = 0: \; A_1(\pm) = \frac{1}{239695200R_e} \left[-2755743930R_e \pm 7830\sqrt{21R_e}\left(-26405533440B_1 - 2805569379R_e + 9013504B_1^2R_e\right)^{\frac{1}{2}}\right]. \tag{71}$$

Unfortunately, this is the maximum progress achieved without specifying the values for the Reynolds number R_e. Namely, in order to get the allowed B_1's, the A_1's from equation (69) must be equated with the A_1 from equation (68). The resulting equation is quadratic for each of the two B_1's, yielding altogether four B_1's as well as four A_1's. As a consequence, there are four sets of coefficients: $A_1, A_2, A_3, A_4; B_1, B_2, B_3, B_4$. However, for R_e between 0 and 1,000, only two sets are real, while the other two sets are complex; only real coefficients can define the

Stokes stream function. Furthermore, since only one set of these coefficients is calculated in the literature [1, 4] and two independent solutions for the Stokes stream function are offered, this approach shows definite progress in this respect. Also, the single set solutions for the coefficients differ numerically between references [1] and [4] as well as with the author's precise calculations, which employed the third edition of Mathematica package [5].

Specifying the Reynolds number R_e, Table 1 presents the calculations of pairs of real A_1, B_1, only; the rest of the corresponding real coefficients $A_2, A_3, A_4; B_2, B_3, B_4$ can then be obtained from equation (66).

Table 1. Calculated Coefficients A_1 and B_1 for Two Numerical Solutions, I and II, of the Navier-Stokes Equation by Galerkin Method. Here, the Reynolds Number Is Varied Between 1 and 10,000

	I		II	
R_e	A_1	B_1	A_1	B_1
1	–4.49912	–0.188993	22.6882	2931.63
10	–4.41227	–1.89842	20.057	309.868
20	–4.41547	–3.84605	16.645	171.199
30	–3.7452	–5.87988	14.2733	126.176
40	–3.21602	–8.00948	12.6375	103.969
50	–1.98757	–10.2042	11.459	90.7646
60	–1.98757	–12.3967	10.5744	82.0239
70	–1.38407	–14.507	9.88776	75.8178
80	–0.830554	–16.4721	–9.34022	71.1879
90	–0.338676	–18.2581	8.52323	67.7492
100	0.0911558	–19.8578	8.52323	67.7492
150	1.53085	–25.5462	7.33534	56.2674
200	2.30045	–28.8338	6.6967	52.0863
400	3.46462	–34.1918	5.68153	45.9191
800	4.03814	–37.0206	5.14878	42.8967
1,000	4.15159	–37.5961	5.04031	42.2982
10,000	4.55591	–39.6918	4.64482	40.1622

In terms of these coefficients, expressions for velocity components can also be obtained now by carrying the differentiation in equations (3) and (4). The results are as follows:

$$u_r = \frac{U}{2\rho^6}\left\{4\left[A_4 + \rho\left(A_3 + A_2\rho + A_1\rho^2\right)\right]\cos\theta + \left[B_4 + \rho\left(B_3 + B_2\rho + B_1\rho^2\right)\right]\left[1 + 3\cos 2\theta\right]\right\}, \quad (72)$$

and

$$u_\theta = \frac{U}{\rho^6} \times \left[-\frac{\rho^6}{\sin\theta} + \left(4A_4 + \rho\left(3A_3 + 2A_2\rho + A_1\rho^2\right) + \left(4B_4 + \rho\left(3B_3 + 2B_2\rho + B_1\rho^2\right)\right)\cos\theta\right)\sin\theta\right]. \quad (73)$$

Utilizing equation (66), these equations can be rewritten in terms of just A_1 and B_1. The result is as follows:

$$\psi = a^2 U \sin^2\theta \left\{\begin{array}{l} \dfrac{\rho^2}{2} + \left[\dfrac{-95 - 34A_1}{58\rho^4} + \dfrac{9(17 + 7A_1)}{29\rho^3} - \dfrac{15(8 + 5A_1)}{29\rho^2} + \dfrac{A_1}{\rho}\right] \\ + \left[-\dfrac{5B_1}{9\rho^4} + \dfrac{19B_1}{9\rho^3} - \dfrac{23B_1}{9\rho^2} + \dfrac{B_1}{\rho}\right]\cos\theta \end{array}\right\}, \quad (74)$$

$$u_r = \frac{1}{261\rho^6} \times \left\{U \times \left[\begin{array}{l} -29B_1(-1+\rho)^2(-5+9\rho) \\ +9\left(-95 + 306\rho - 240\rho^2 + 2A_1(-1+\rho)^2(-17+29\rho)\right)\cos\theta \\ +87B_1(-1+\rho)^2(-5+9\rho)\cos^2\theta \end{array}\right]\right\}, \quad (75)$$

and

$$
u_\theta = -\frac{1}{\rho} \times \left\{ \begin{array}{l} \dfrac{U}{\sin\theta} \\ \times \left[\rho - \dfrac{1}{261\rho^5} \left(\left(\begin{array}{l} 9\left(-190 + 459\rho - 240\rho^2 + A_1\left(-68 + 189\rho - 150\rho^2 + 29\rho^3\right)\right) + \\ + 29B_1\left(-20 + 57\rho - 46\rho^2 + 9\rho^3\right)\cos\theta \end{array} \right) \sin^2\theta \right) \right] \end{array} \right\}. \tag{76}
$$

It has been known for quite some time that the Navier-Stokes equation has a steady solution with the standard coefficients from Table 1 (denoted as I) when the Reynolds number is below the critical point. In references [1] and [4], the critical Reynolds number is deduced to be about 100. Beyond this number, the steady flow becomes superimposed with secondary flows and/or flows with vortices that become dominant as the Reynolds number approaches 1,000, as indicated by Chow [6]. On the other hand, Kawaguti [4] claims that the solution for ψ (with the standard coefficients) describes a steady flow only for $10 < R_e < 80$. At $R_e = 100$ and beyond, the flow becomes unstable and periodic and transforms itself into flow with von Karman's vortex-street or with distorted loops of vorticity arranged with some measure of symmetry.

Unfortunately, as the Reynolds number increases further (to 1,000 and beyond), the standard solution for ψ becomes more difficult to connect to experiments. In fact, Kawaguti [4] has found that even when the Reynolds number is increased indefinitely, the Galerkin method with the standard coefficients (I) would predict a steady solution for the Navier-Stokes equation, although it could not be found experimentally. For this reason, it is necessary to study the solutions to the Navier-Stokes equation, with the Galerkin method utilizing the second coefficients (II). It is possible that, since coefficients I and II are distinctly different, the physics of the flow will also be different. Hence, more than likely, the solution of the Navier-Stokes equation with the coefficients II will describe the turbulent flow which, in turn, should correspond to the fluid breakup.

Finally, the stability of the solutions, either with the coefficients I or II, should be investigated by the perturbation method. Here, following Kawaguti [4], an exponential in time

perturbation is added to the steady solution, and whether this perturbation grows or disappears is studied. If it grows, then an unstable solution indicates the likely fluid breakup.

4. Examples of Applications of the New and Standard Solutions of the Navier-Stokes Equation

Concerning the type I coefficients entering into the Galerkin method solution for the Navier-Stokes equation, by using a special type of perturbation, Kawaguti [4] deduced that the critical Reynolds number (below which the airflow around the spherical fluid is steady) is about 51. Experimentally, however, it is known to be around 100 and beyond, depending on the fluid. Also, the type I coefficients, while reproducing the calculated drag in a fair agreement with experiments, fail to do so for vorticity and pressure distributions over the spherical fluid surface [4].

These facts alone should be enough to pursue the solution for the Navier-Stokes equation using the Galerkin method with the type II coefficients.

Figures 2–7 describe examples of angular dependencies of ψ, u_r, and u_θ at $R_e = 1{,}000$, $r = 2a$, $a = 1\,m$, and $U = 30\,ms$ with type I and II coefficients. In specific evaluations, when determining R_e, the viscosity μ and the air density ρ would have to be taken explicitly into account. Nevertheless, it is easily seen from these examples that graphs with coefficients II describe a different physical situation than the graphs with the coefficients I. Hence, the author believes that the solution with the type II coefficients could very well be more appropriate to describe the fluid breakup at very high (sonic) velocities of the fluid in the air.

5. Conclusion and Recommendations

Although much has been accomplished in this report when evaluating the stream functions and velocity components around the spherical fluid, more could and should be done. In particular, evaluations of the drag coefficients of the sphere, as well as the vorticity and pressure

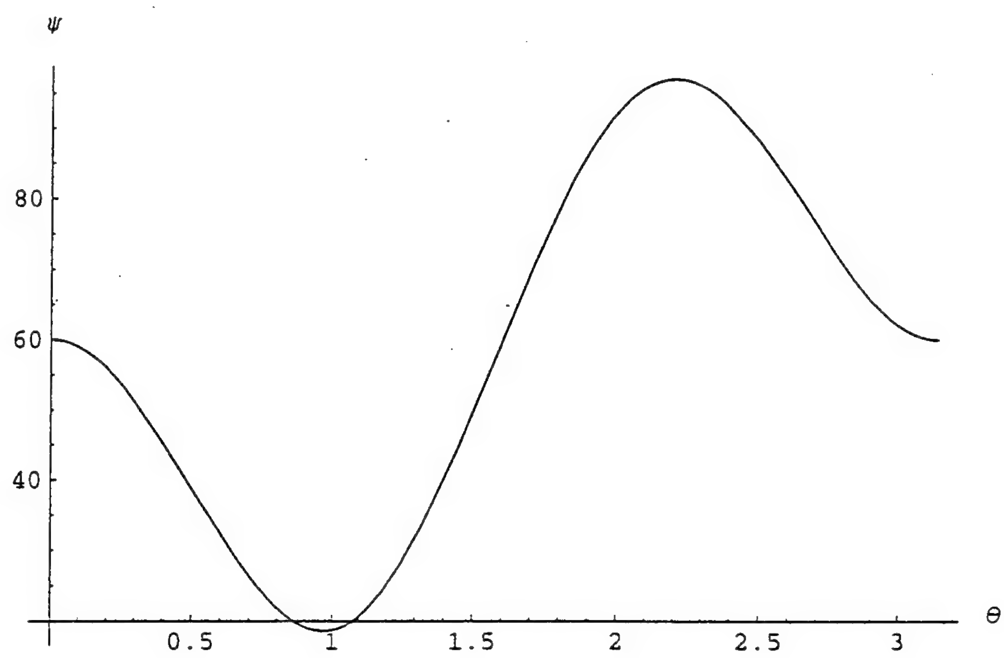

Figure 2. Example of the Angular Dependence of the Stokes Stream Function ψ Around the Spherical Fluid. It Was Evaluated With Coefficients I at $R_e = 1{,}000$, $r = 2a$, $a = 1$ m, and $U = 30\ ms^{-1}$.

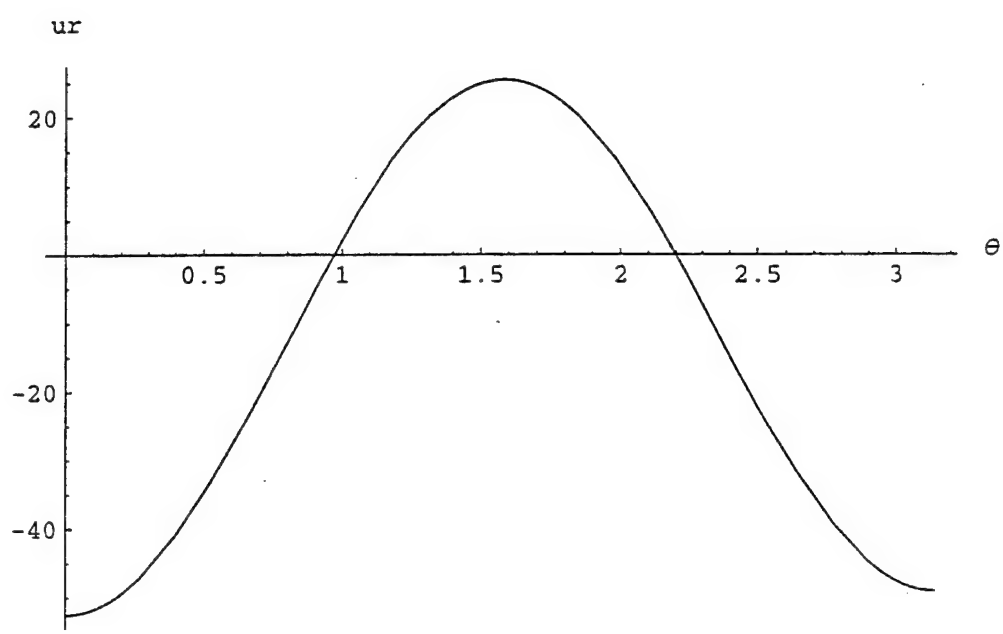

Figure 3. Example of the Angular Dependence of the Radial Component of the Air Element Velocity u_r Around the Spherical Fluid. It Was Evaluated With Coefficients I at $R_e = 1{,}000$, $r = 2a$, $a = 1$ m, and $U = 30\ ms^{-1}$.

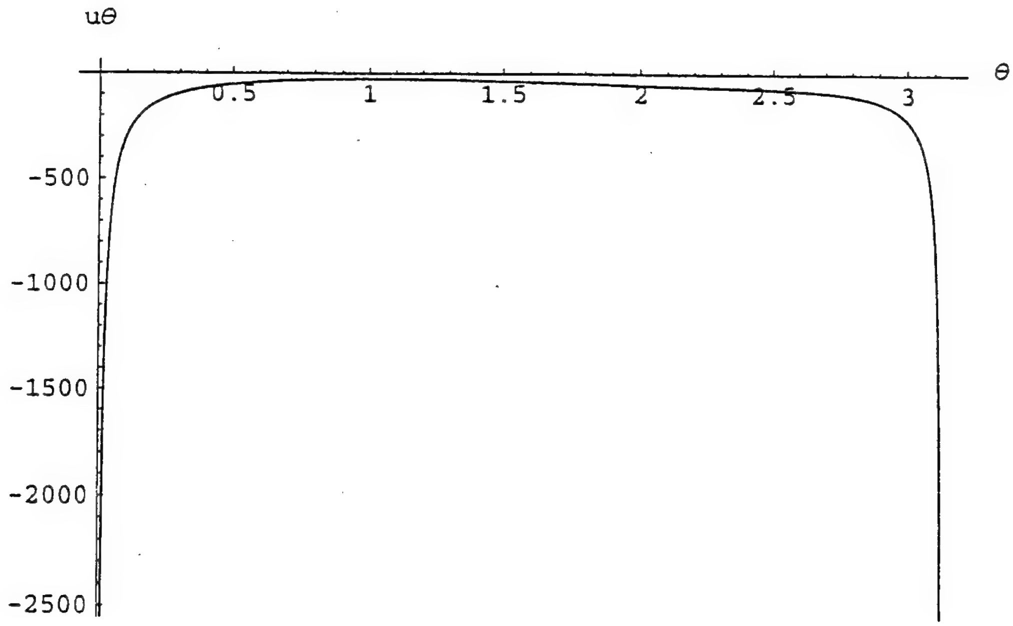

Figure 4. Example of the Angular Dependence of the Angular Component of the Air Element Velocity u_θ Around the Spherical Fluid. It Was Evaluated With Coefficients I at $R_e = 1{,}000$, $r = 2a$, $a = 1$ m, and $U = 30\ ms^{-1}$.

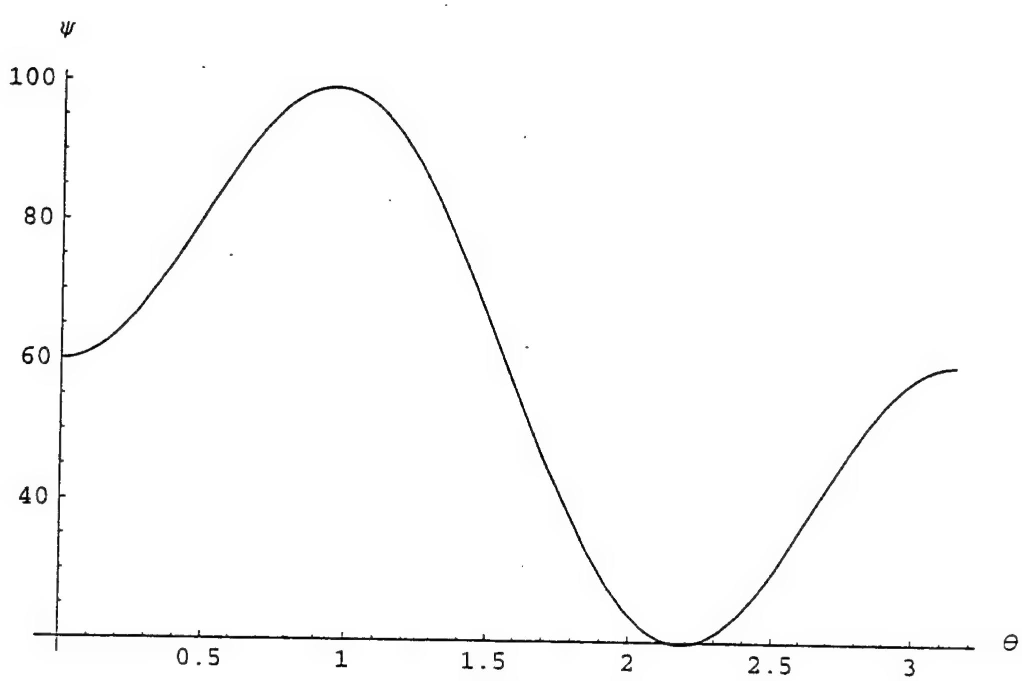

Figure 5. Example of the Angular Dependence of the Stokes Stream Function ψ Around the Spherical Fluid. It Was Evaluated With Coefficients II at $R_e = 1{,}000$, $r = 2a$, $a = 1$ m, and $U = 30\ ms^{-1}$.

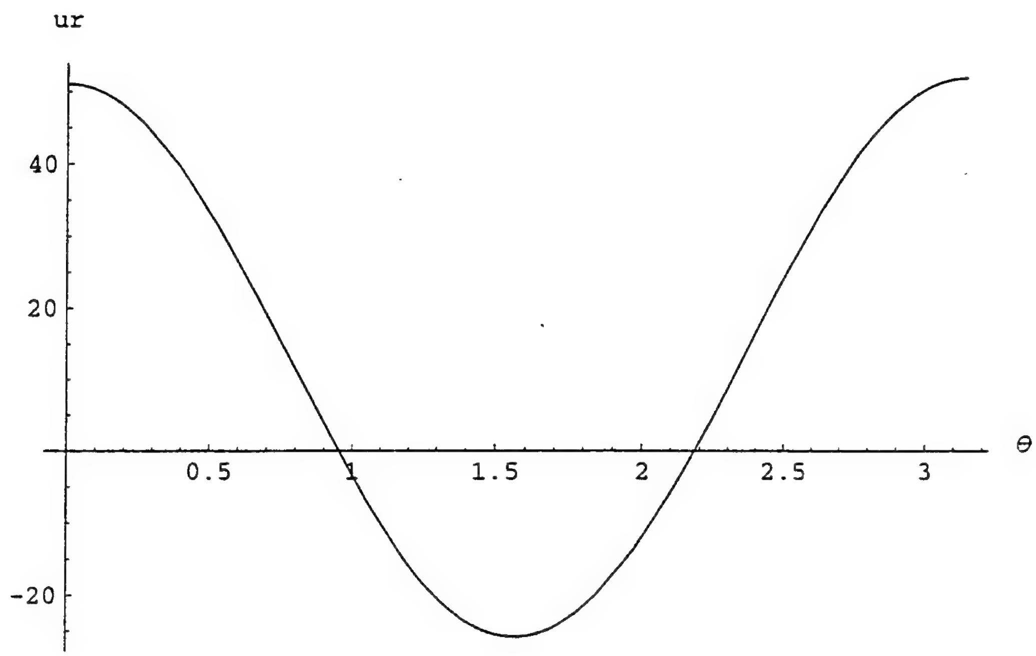

Figure 6. Example of the Angular Dependence of the Radial Component of the Air Element Velocity u_r Around the Spherical Fluid. It Was Evaluated With Coefficients II at $R_e = 1{,}000$, $r = 2a$, $a = 1$ m, and $U = 30\ ms^{-1}$.

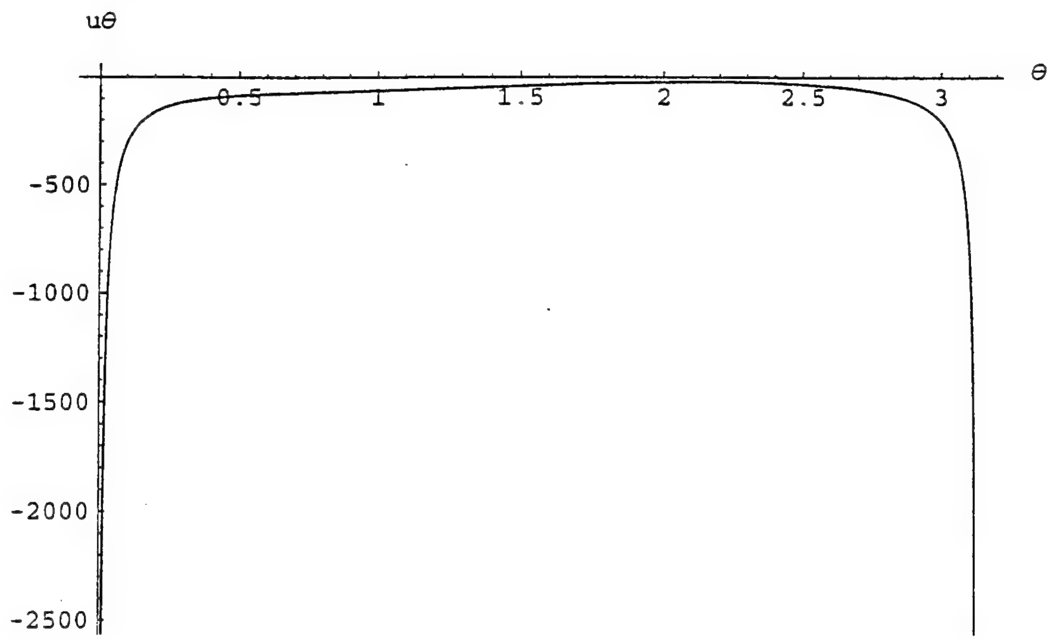

Figure 7. Example of the Angular Dependence of the Angular Component of the Air Element Velocity u_θ Around the Spherical Fluid. It Was Evaluated With Coefficients II at $R_e = 1{,}000$, $r = 2a$, $a = 1$ m, and $U = 30\ ms^{-1}$.

distributions over the spherical surface,. should be done. These would be needed not only to make intelligible comparisons with experiments but also to develop a full picture of the fluid breakup after leaving either a ballistic or cruise missile.

6. References

1. Hughes, W. F., and E. W. Gaylord. *Basic Equations of Engineering Science.* New York: Schaum Publishing Company, 1964.

2. Acheson, D. J. *Elementary Fluid Dynamics*. Oxford, England: Clarendon Press, 1998.

3. Merzbacher, E. *Quantum Mechanics*. New York: John Wiley & Sons, 1970.

4. Kawaguti, M. "The Critical Reynolds Numbers for the Flow Past a Sphere." *Jour. Phys. Japan,* vol. 10, pp. 694–699, 1955.

5. Wolfram, S. *The Mathematica Book.* 3rd edition, Champaign, IL: Wolfram Media and Cambridge University Press, 1996.

6. Chow, C-Y. *An Introduction to Computational Fluid Dynamics*. New York: John Wiley & Sons, 1979.

INTENTIONALLY LEFT BLANK.

NO. OF COPIES	ORGANIZATION
2	DEFENSE TECHNICAL INFORMATION CENTER DTIC OCA 8725 JOHN J KINGMAN RD STE 0944 FT BELVOIR VA 22060-6218
1	HQDA DAMO FDT 400 ARMY PENTAGON WASHINGTON DC 20310-0460
1	OSD OUSD(A&T)/ODDR&E(R) DR R J TREW 3800 DEFENSE PENTAGON WASHINGTON DC 20301-3800
1	COMMANDING GENERAL US ARMY MATERIEL CMD AMCRDA TF 5001 EISENHOWER AVE ALEXANDRIA VA 22333-0001
1	INST FOR ADVNCD TCHNLGY THE UNIV OF TEXAS AT AUSTIN 3925 W BRAKER LN STE 400 AUSTIN TX 78759-5316
1	DARPA SPECIAL PROJECTS OFFICE J CARLINI 3701 N FAIRFAX DR ARLINGTON VA 22203-1714
1	US MILITARY ACADEMY MATH SCI CTR EXCELLENCE MADN MATH MAJ HUBER THAYER HALL WEST POINT NY 10996-1786
1	DIRECTOR US ARMY RESEARCH LAB AMSRL D DR D SMITH 2800 POWDER MILL RD ADELPHI MD 20783-1197

NO. OF COPIES	ORGANIZATION
1	DIRECTOR US ARMY RESEARCH LAB AMSRL CI AI R 2800 POWDER MILL RD ADELPHI MD 20783-1197
3	DIRECTOR US ARMY RESEARCH LAB AMSRL CI LL 2800 POWDER MILL RD ADELPHI MD 20783-1197
3	DIRECTOR US ARMY RESEARCH LAB AMSRL CI IS T 2800 POWDER MILL RD ADELPHI MD 20783-1197
	<u>ABERDEEN PROVING GROUND</u>
2	DIR USARL AMSRL CI LP (BLDG 305)

NO. OF COPIES	ORGANIZATION
1	OASD C3I J BUCHHEISTER RM 3D174 6000 DEFENSE PENTAGON WASHINGTON DC 20301-6000
1	OUSD AT STRT TAC SYS DR SCHNEITER RM 3E130 3090 DEFENSE PENTAGON WASHINGTON DC 20301-3090
1	OUSD(A&T)/S&T AIR WARFARE R MUTZELBUG RM 3E139 3090 DEFENSE PENTAGON WASHINGTON DC 20301-3090
1	OUSD(A&T)/S&T LAND WARFARE A VIILU RM 3B1060 3090 DEFENSE PENTAGON WASHINGTON DC 20310-3090
1	UNDER SECY OF THE ARMY DUSA OR ROOM 2E660 102 ARMY PENTAGON WASHINGTON DC 20310-0102
1	ASST SECY ARMY ACQSTN LOGISTCS & TECHLGY SAAL ZD ROOM 2E673 103 ARMY PENTAGON WASHINGTON DC 20301-0103
1	ASST SECY ARMY ACQSTN LOGISTCS & TECHLGY SAAL ZP ROOM 2E661 103 ARMY PENTAGON WASHINGTON DC 20310-0103
1	ASST SECY ARMY ACQSTN LOGISTCS & TECHLGY SAAL ZS ROOM 3E448 103 ARMY PENTAGON WASHINGTON DC 20310-0103

NO. OF COPIES	ORGANIZATION
1	OADCSOPS FORCE DEV DIR DAMO FDZ ROOM 31522 460 ARMY PENTAGON WASHINGTON DC 20301-0460
1	HQDA ODCSPER DAPE MR RM 2C733 300 ARMY PENTAGON WASHINGTON DC 20301-0300
1	US ARMY ARMAMENT RDEC AMSTA AR TD M FISETTE BLDG 1 PICATINNY ARSENAL NJ 07806-5000
1	US ARMY MISSILE RDEC AMSMI RD DR W MCCORKLE REDSTONE ARSENAL AL 35898-5240
1	NATICK SOLDIER CENTER SBCN T P BRANDLER KANSAS STREET NATICK MA 01760-5056
1	US ARMY TANK AUTOMTV RDEC AMSTA TR J CHAPIN WARREN MI 48397-5000
1	US ARMY INFO SYS ENGRG CMD AMSEL IE TD DR F JENIA FT HUACHUCA AZ 85613-5300
1	US ARMY SIM TRNG INST CMD AMSTI CG DR M MACEDONIA 12350 RESEARCH PKWY ORLANDO FL 32826-3726
1	US ARMY TRADOC BATTLE LAB INTEGRATION TECH & CONCEPTS DIR ATCD B FT MONROE VA 23651-5850

NO. OF COPIES	ORGANIZATION
1	US ARMY TRADOC ANL CTR ATRC W A KEINTZ WSMR NM 88002-5502
1	US ARMY RESEARCH OFFICE 4300 S MIAMI BLVD RESEARCH TRIANGLE PARK NC 27709
1	US ARMY RESEARCH LAB AMSRL SL C HOPPER WSMR NM 88002-5513
1	US ARMY RESEARCH LAB AMSRL SL E J PALOMO WSMR NM 88002-5513
1	US ARMY RESEARCH LAB AMSRL SL EA R FLORES WSMR NM 88002-5513
1	US ARMY RESEARCH LAB AMSRL SL EI J NOWAK FT MONMOUTH NJ 07703-5601
	ABERDEEN PROVING GROUND
1	SBCCOM RDEC AMSSB RTD J ZARZYCKI 5183 BLACKHAWK RD APG MD 21010-5424
1	US ARMY DEV TEST COM CSTE DTC TT T APG MD 21005-5055
1	US ARMY EVALUATION CENTER CSTE AEC W HUGHES 4120 SUSQUEHANNA AVE APG MD 21005-3013

NO. OF COPIES	ORGANIZATION
1	US ARMY EVALUATION CENTER CSTE AEC SV L DELATTRE 4120 SUSQUEHANNA AVE APG MD 21005-3013
	ABERDEEN PROVING GROUND (CONT)
14	DIR USARL AMSRL SL DR WADE J BEILFUSS AMSRL SL B J SMITH J FRANZ M VOGEL W WINNER AMSRL SL BA M RITONDO AMSRL SL BD J MORRISSEY AMSRL SL BE D BELY AMSRL SL BG A YOUNG AMSRL SL BN D FARENWALD AMSRL SL E M STARKS AMSRL SL EC E PANUSKA AMSRL SL EM J FEENEY

NO. OF COPIES	ORGANIZATION
	ABERDEEN PROVING GROUND
22	DIR USARL AMRSL SL BN J SOLN (20 CPS) AMSRL SL EA R ORTEGA B RUTH

REPORT DOCUMENTATION PAGE

Form Approved
OMB No. 0704-0188

1. AGENCY USE ONLY *(Leave blank)*	2. REPORT DATE	3. REPORT TYPE AND DATES COVERED
	June 2001	Final, October 1997–January 2000

4. TITLE AND SUBTITLE
Modeling of a Fluid Breakup Through Nonlinear Fluid Flow: Description of Methodology

5. FUNDING NUMBERS
665604D670

6. AUTHOR(S)
Josip Z. Šoln

7. PERFORMING ORGANIZATION NAME(S) AND ADDRESS(ES)
U.S. Army Research Laboratory
ATTN: AMSRL-SL-BN
Aberdeen Proving Ground, MD 21010-5423

8. PERFORMING ORGANIZATION REPORT NUMBER
ARL-TR-2543

9. SPONSORING/MONITORING AGENCY NAMES(S) AND ADDRESS(ES)

10.SPONSORING/MONITORING AGENCY REPORT NUMBER

11. SUPPLEMENTARY NOTES

12a. DISTRIBUTION/AVAILABILITY STATEMENT
Approved for public release; distribution is unlimited.

12b. DISTRIBUTION CODE

13. ABSTRACT *(Maximum 200 words)*

Employing the Galerkin method, we find altogether four solutions for the Navier-Stokes equation describing the airflow around a fluid sphere. Two solutions are real, and two are complex. Of the two real solutions, one is a standard solution described by Kawaguti some time ago. A new real solution is distinctly different from the standard one and, as such, gives a qualitatively different description of the flow around a sphere. For large Reynolds numbers, this new solution should be appropriate for deducing the critical forces on the fluid sphere responsible for its breakup.

14. SUBJECT TERMS
modeling, fluid breakup methodology

15. NUMBER OF PAGES
37

16. PRICE CODE

17. SECURITY CLASSIFICATION OF REPORT	18. SECURITY CLASSIFICATION OF THIS PAGE	19. SECURITY CLASSIFICATION OF ABSTRACT	20. LIMITATION OF ABSTRACT
UNCLASSIFIED	UNCLASSIFIED	UNCLASSIFIED	UL

NSN 7540-01-280-5500

Standard Form 298 (Rev. 2-89)
Prescribed by ANSI Std. 239-18 298-102

INTENTIONALLY LEFT BLANK.

USER EVALUATION SHEET/CHANGE OF ADDRESS

This Laboratory undertakes a continuing effort to improve the quality of the reports it publishes. Your comments/answers to the items/questions below will aid us in our efforts.

1. ARL Report Number/Author ARL-TR-2543 (Šoln) ________ Date of Report June 2001 ________

2. Date Report Received ________________________________

3. Does this report satisfy a need? (Comment on purpose, related project, or other area of interest for which the report will be used.) ________________________________

____

4. Specifically, how is the report being used? (Information source, design data, procedure, source of ideas, etc.) ________

____

____

5. Has the information in this report led to any quantitative savings as far as man-hours or dollars saved, operating costs avoided, or efficiencies achieved, etc? If so, please elaborate. ________________________________

____

____

6. General Comments. What do you think should be changed to improve future reports? (Indicate changes to organization, technical content, format, etc.) ________________________________

____

____

____

CURRENT ADDRESS

____
Organization

____
Name E-mail Name

____
Street or P.O. Box No.

____
City, State, Zip Code

7. If indicating a Change of Address or Address Correction, please provide the Current or Correct address above and the Old or Incorrect address below.

OLD ADDRESS

____
Organization

____
Name

____
Street or P.O. Box No.

____
City, State, Zip Code

(Remove this sheet, fold as indicated, tape closed, and mail.)

(DO NOT STAPLE)